

Voice-coil array development for a deformable mirror

Ryan Luder, Michael Hart, Krysta Pavlica, and Olivia Fehlberg

University of Arizona, College of Optical Sciences, 1630 E University Blvd, Tucson, AZ 85721

ABSTRACT

Voice-coil actuators are an attractive choice for deformable mirror (DM) drivers given their inherently large stroke and relatively low cost scaling. In this paper, we describe the construction of a prototype DM composed of seven actuators mounted behind a deformable face sheet. For the electro-mechanical tests reported here, an aluminum face sheet has been used. In future this will be replaced by glass. The control system for the voice coils involves an EtherCAT framework, which paired with Ingenia motion controllers allows for kHz operation rates. The intent in this project is to perform correction without the need for position sensors on the mirror, requiring low hysteresis effects in the motion of the coils. To this end, a 3D printed flexure was designed to reduce frictional effects on the coils' motion, as well as set a constant zero-current position. The position of the coils as a function of force input is characterized using capacitive sensor measurements, with an analysis of residual hysteresis and noise. The current status of the project as well as its viability for scaling to larger actuator counts and mirrors is discussed.

Keywords: Deformable mirrors, adaptive optics

1. INTRODUCTION

Telescopes that make use of adaptive optics systems are growing both in popularity and in size. Correspondingly, the drive to make use of technologies that are cost-effective and scalable is also increasing, especially in the case of deformable mirror (DM) drivers. Of the various actuator technologies, voice-coils are an attractive choice for deformable mirror drivers due to several unique qualities. These motors are composed of a current coil that influences an interior magnet, such that the output force applied varies linearly with current. Voice-coil driven DM's as opposed to piezo actuator DM's have larger stroke available for wavefront correction, and tend to be more easily scalable due to the simplicity of their design. In addition, a single failed actuator in an array still moves freely when under force, and is not pinned in place. For these reasons, voice-coil driven deformable mirrors have been used successfully in adaptive secondaries such as the MMT¹ as well as in smaller scale systems². In these examples, the motion of the mirror is controlled through feedback from individual position sensors coupled to each actuator which regulate the servo. While this configuration performs effectively, the added necessity of positions sensors attached to each motor introduces complexity and expense to the system, especially considering the increasing number of actuator counts.

In this paper, we describe the development and performance of a prototype seven-actuator DM that operates without the need for position sensors attached to each voice-coil. Instead, the DM's construction was designed to linearize the motion of the mirror to the point where prediction-based motor position was sufficient. To this end, the system was engineered to dramatically reduce hysteresis inherent in the motors. This hysteresis arises due to contact between the outer coil and the inner magnet of the VC, and can only be eliminated by orienting the magnet in a way that it is 'floating' centrally within the motor housing. This problem was resolved by the use of a low-cost 3D printed flexure, which is described further in section 2. For testing, the DM was fitted with an aluminum face sheet with a capacitive position sensor. Current results show a high degree of linearity and low residual hysteresis in the motion of the DM, which indicate good chances for wavefront correction in future testing, though the system is noise-limited in

smaller ranges of DM motion. With the reduction of noise in the current sensing, we believe that our prototype DM will serve as a highly scalable, low cost/complexity option for increasingly large secondaries.

2. CONSTRUCTION

2.1 System Overview

Fig. 1 below shows the completed design of the prototype, which consists of the invar 36 mount, voice-coil array, flexure, and 3 inch diameter aluminum face sheet. The coils used here were purchased from H2W Technologies, with part # NCM01-05-003-3X. There are seven voice-coils in total, six of which are arranged in hexagonal fashion around a centrally oriented coil. This geometry allows the face sheet to express several of the low-order zernike modes such as focus, astigmatism, etc. The center magnet of each coil is fixed to a cylindrical pin, which is in turn epoxied to the aluminum face sheet. The total stroke of each actuator is 2.5 mm, and has an electrical time constant of 0.06 ms which is acceptable for kHz speed wavefront correction. The face sheet is attached to a small aluminum flexure in addition to the voice coils, allowing for smooth tip-tilt motion during the operation of the mirror. It should be noted that this flexure is separate from the printed flexure designed for hysteresis reduction described in section 2.3.

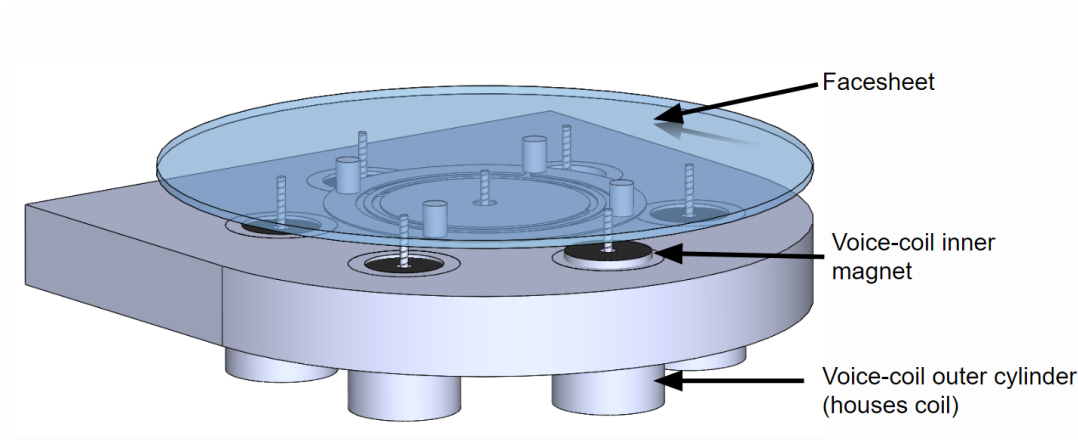


Figure 1. Model of the face sheet, mount, and VC array. A glass face sheet is displayed for visibility, though an aluminum flat is used for testing.

Because the control mechanism of the voice coils is unregulated by position sensors and servos on force alone, the face sheet transfer function from voice-coil current to position is highly dependent on the material characteristics of the face sheet itself. The testing described in section 3 has been performed on an aluminum face sheet, with the intention of changing to a 1 mm thick glass face sheet with reduced stiffness. Aluminum serves as a good intermediate testing material due to its ease of use with capacitive sensors, as well as its mechanical similarity to glass. The transfer function is also dependent on the printed flexure which can be seen in Fig. 2 opposite the face sheet. This flexure was designed to centrally constrain the voice coil magnets with little influence on the motion of the voice coils parallel to the mirror's normal vector. This influence is non-zero however, and nonlinear effects can be seen at the extreme ranges of voice-coil motion.

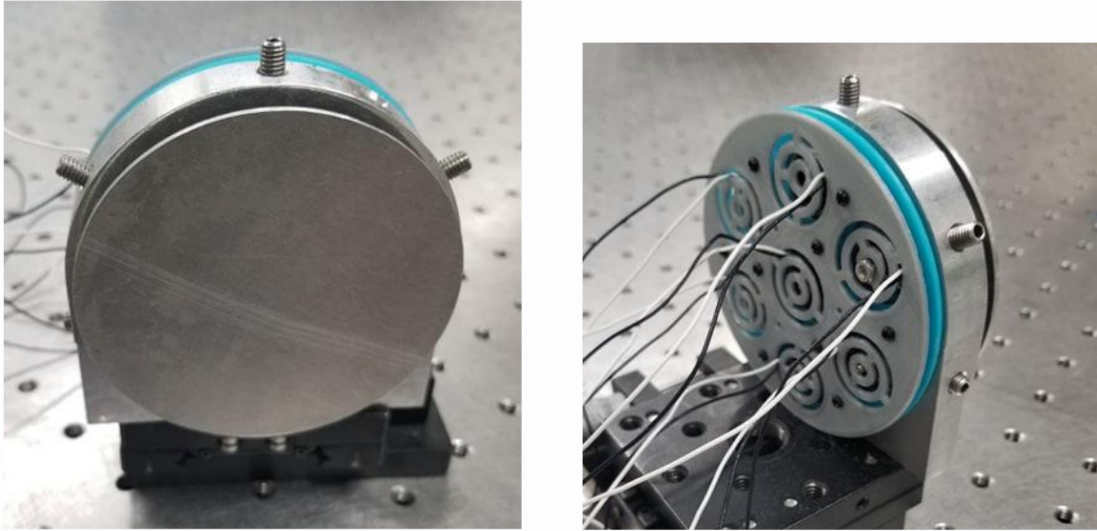


Figure 2. Images of the deformable mirror with the aluminum face sheet (left) and printed flexure attached (right). The voice-coils are hidden behind each circular pattern of the flexure.

2.2 Control Scheme

Each of the seven voice-coils have an output force which is directly proportional to the input current provided by seven corresponding Ingenia Neptune motion control drivers. When operating in a force servo, a hall-effect current sensor onboard each driver forms the basis of the voice-coil feedback. With further development, a given force-based transfer function can be converted into position assuming a Hooke's law behavior of the face sheet with small deformations. This transfer function is likely to vary with different zernike orders, as similar stroke for higher spatial frequencies should require more applied force to produce. With interferometric testing, these transfer functions can be modelled numerically³. This scheme allows for position-based control without the use of position sensors themselves, which add expense and complexity to any AO system.

As Windows devices are not real-time systems in general and standard USB connections are subject to timing jitter and high latency, a Beckhoff EtherCAT fieldbus control setup was chosen for the operation of the DM. This involves a standard master-slave configuration in which the seven slaves are daisy-chained in sequence, as shown in Fig. 3. The direct hardware commands are sent through TwinCAT software for ease of communication over EtherCAT devices. However, forces and positions are manipulated in Matlab for easier interfacing with wavefront sensing as well as matrix calculations.

With this control scheme, we expect to be able to generate multiple low order zernike polynomials on the face sheet, with amplitudes dependent on the face sheet material chosen. Ultimately we are limited in the figures we can produce by the maximum three actuator sampling across the diameter. The selected hardware and software are all capable of providing at least kHz update rates and with negligible communication delay between each of the seven actuators.

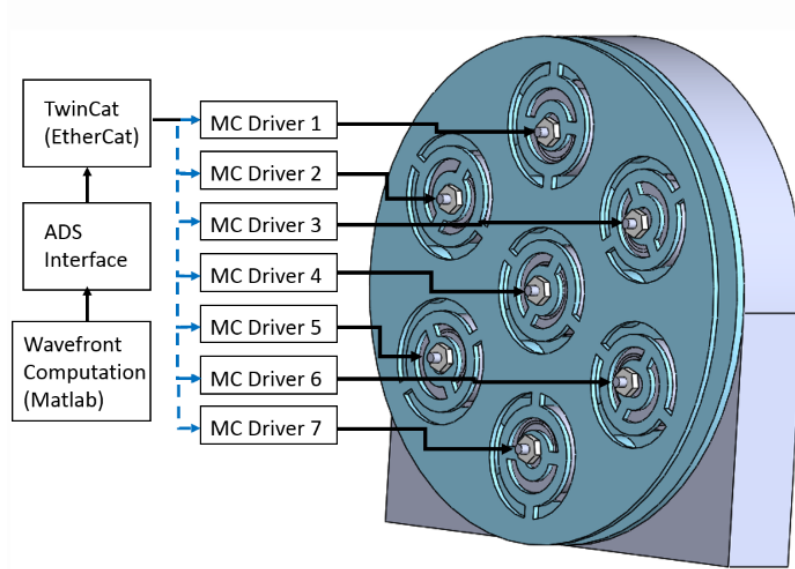


Figure 3. Schematic of the DM control layout. The connection from driver to motor is through an applied DC current for static position demands.

2.3 Hysteresis Reduction

The efficacy of controlled motion without the use of position sensors is highly dependent on having a system with little hysteresis. The mechanical design is therefore tailored to avoid hysteresis. With the DM oriented vertically, the natural position of the inner magnet within each voice-coil is to rest on the bottom surface of the coil. This position generates friction-based hysteresis that presents as ‘stiction,’ where the position of the motor slips unpredictably forward once a minimum threshold of force is applied. The magnetic section of the motor needs to be freely suspended centrally in the coil to eliminate this effect. This was accomplished through the development of a 3D printed flexure displayed in Fig. 4, which shows the flexure itself and an FEA model of one voice-coil’s deformation. The flexure is composed of a base which is fixed onto the DM mount, and a thin ABS sheet. Seven circular patterns which correspond to each voice-coil are cut into this sheet, which is fixed to the base opposite the face sheet and shares the same 3 inch diameter geometry. The patterns are designed to constrain the pin of the voice-coil centrally, with limited effect on motion in the direction of the face sheet normal vector. Specifically, the patterns should not cause unwanted rotation or angular deflection within the range of the voice-coil. In practice, some opposition and deflection occur in the far reaches of the stroke of each motor, which produce nonlinearities in the hysteresis curve at those positions.

After the implementation of the flexure, the frictional effects on the voice-coil motion were significantly reduced, as described in section 3. An added benefit of this change is a reduction in piston variation with changes in orientation, due to the restoring force provided by the flexure. So far the flexure has performed well with static capacitive sensor testing of single actuator position. More work is necessary to judge the performance with multiple actuators moving simultaneously, and at kHz speeds.

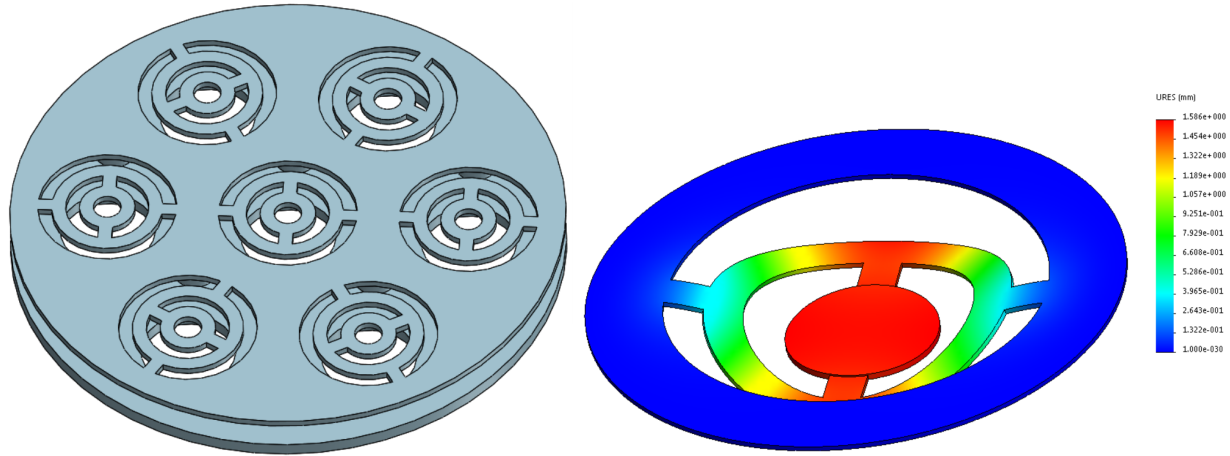


Figure 4 (Left.) The base and patterned flexure that form the constraining mechanism for the voice-coils. (Right.) Finite element analysis of an individual pattern with a single voice-coil's applied force.

3. RESULTS

The linearity of the face sheet deflection was tested using a capacitive sensor placed opposite a single voice-coil and adjacent to the aluminum face sheet. The data shown below in Fig. 5 are the result of time-averaging the capacitive sensor reading at static displacements. For this test, only a single voice-coil is actuated while the six other actuators are allowed to move freely. The averaging is performed at each 5 mN force increment, and consists of 100 samples before the next increase in applied force. This process is intended to reduce noise inherent to the driver's hall-effect sensor, and to better emphasize the linearity and low hysteresis of the motors. Four forward-backward cycles of motion are displayed in this example, with each cycle being performed over a 160 second period, for a total length of 21.3 minutes.

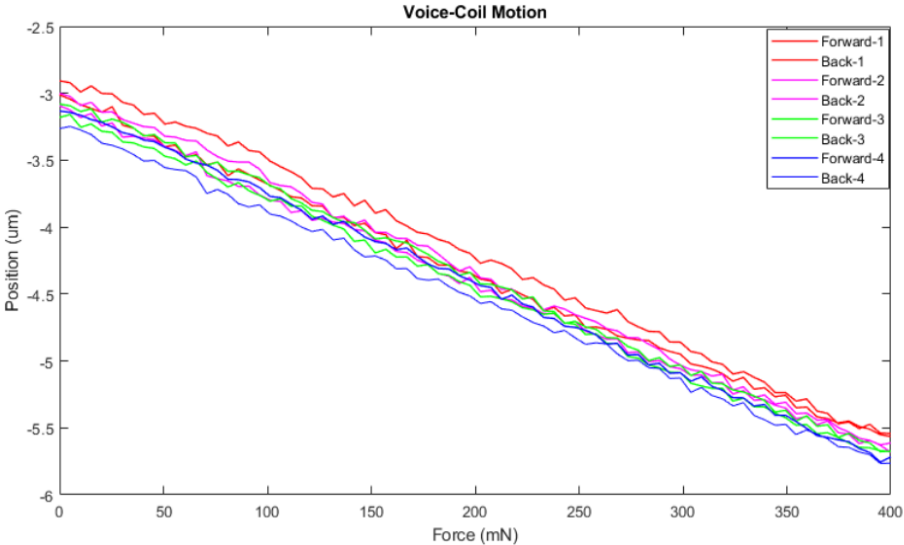


Figure 5. Face sheet deformation as a result of single actuator force. The force is incremented and measured statically, as well as heavily averaged at each force value to reduce the effects of the noisy current sensor.

The data shown above displays a high degree of linearity compared to the quadratic ‘stiction’ motion seen without the use of the flexure. Linear fits of the forward and backward motion are shown in Figs. 6 and 7, and the corresponding statistics of each fit are in Table 1 below.

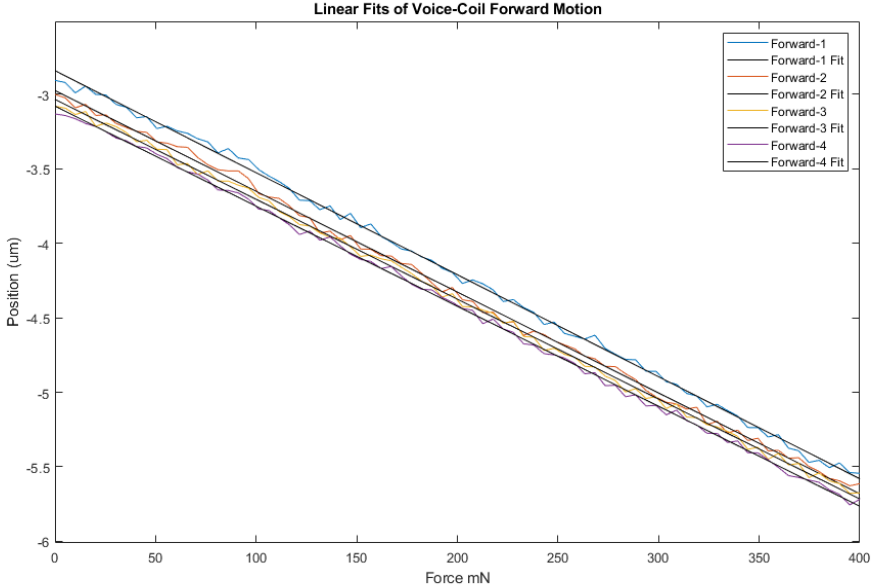


Figure 6. Linear fit of the forward half of each voice-coil cycle.

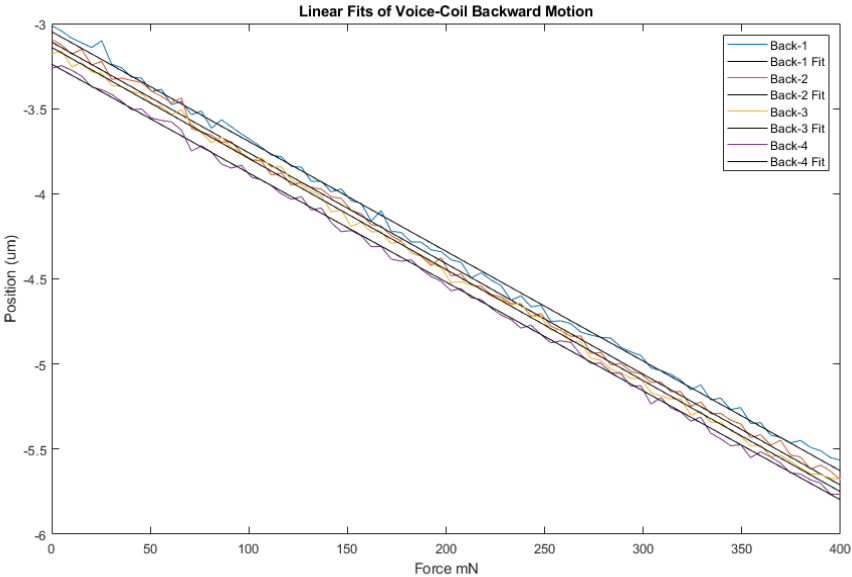


Figure 7. Linear fit of the backward half of each voice-coil cycle.

Forward Motion	Slope (nm/mN)	Position Intercept (μm)	RMSE (μm)
1	-6.85	-2.84	2.93E-02
2	-6.76	-2.97	2.96E-02
3	-6.70	-3.03	2.62E-02
4	-6.71	-3.08	2.15E-02
Backward Motion			
1	-6.45	-3.05	3.43E-02
2	-6.51	-3.11	3.25E-02
3	-6.53	-3.14	2.72E-02
4	-6.40	-3.24	2.46E-02

Table 1. Fitting statistics for the plots in Figs. 6 and 7. The position intercept in this table refers to the 0 mN intercept of both the forward and backward cycle fit, rather than the starting position of the motion.

Higher order polynomial fits were also attempted for the above datasets to determine if any of the quadratic motion associated with frictional forces remained after correction. However, all coefficients associated with higher than linear order motion were at least three orders of magnitude below the linear coefficient.

By far, the largest error in the mirror's motion is the noise level of the hall-effect current sensor within the driver. Ingenia's Neptune MC driver has a stated accuracy of 1% of the full range of its 6.3 A output. With the 2.3 N/A force constant of the voice-coils and assuming a 7 nm/mN slope, this error can produce a peak deviation of 1 micron from the command given. Experimentally, this current noise error presents as 190 nm rms position noise that is independent of PID control, which can only be effected through averaging.

Some low frequency hysteresis was observed with subsequent cycles of motion, as can be seen in the drift of the position intercepts in Table 1. The mean hysteresis of this kind is 0.17 μm per 320 second cycle, or 32 nm per minute. Some amount of drift is expected as the coils dissipate 70 mW of power at 400 mN, and the voice-coils do not have a dedicated cooling mechanism currently beyond passive contact with the mount. Therefore, changes in position with thermal expansion is likely.

In the future, we intend to replace the aluminum face sheet with glass. This will allow for interferometric tests of a surface driven by all seven actuators simultaneously, and to investigate the practical application of prediction-based motion without the use of position sensors coupled to each actuator. Several of the low order Zernike modes that can be produced using seven actuators are shown below in Fig. 8. These surfaces were produced using a finite-element analysis of a glass face sheet under the influence of seven corresponding actuators. In addition, we would like to reduce the position noise visible in Fig. 5 which is due to the hall-effect sensor onboard the Ingenia driver. These drivers will need to be replaced with a higher fidelity current source in future. At present, the existing noise limits the possibility of wavefront correction with a glass face sheet.

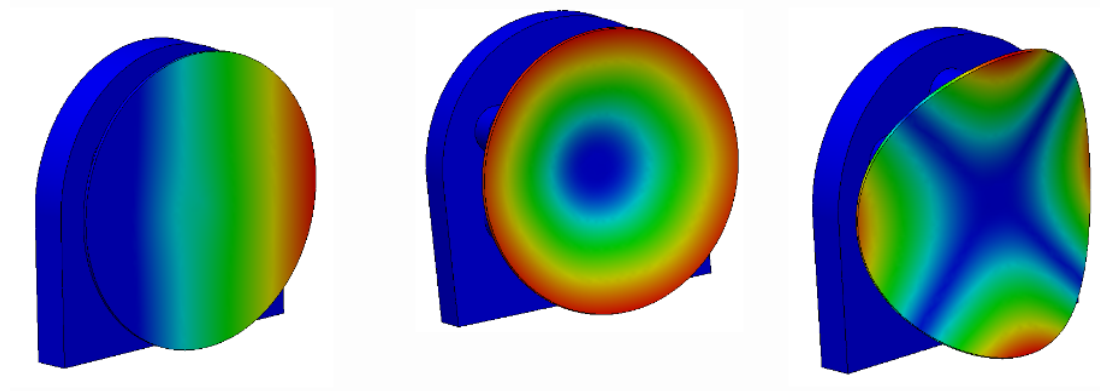


Figure 8. FEA simulation of glass material under the influence of seven actuators. Tilt, defocus, and astigmatism are three of the zernike orders that can be produced using a low actuator count.

4. DISCUSSION

We believe that our prototype deformable mirror has demonstrated the linear behaviour required for a system operating without the use of position sensors. The flexure has reduced the hysteresis of the coils to a level where thermal drift is the dominant factor of their time-dependence. In order to claim that the system is fully ready for wavefront correction however, some further design issues need to be addressed. The noise inherent to the driver's hall-effect current sensor is the primary issue, as its position variance currently exceeds the expected phase errors we would need to correct. The aluminum face sheet must be replaced with glass, so interferometric testing can take place. Finally, the transfer function for current-position operation must be characterized for multiple zernike orders, using the above interferometric results.

REFERENCES

- [1] Wildi, Francois P, Guido Brusa, Armando Riccardi, Michael Lloyd-Hart, Hubert M Martin, and Laird M Close. "Towards First Light of the 6.5m MMT Adaptive Optics System with Deformable Secondary Mirror." 4839.1 (2003): 155-63.
- [2] Wildi, François P, Gabriel Mühlebach, and Tony Maulaz. "Low Order High Accuracy Deformable Mirror Based on Electromagnetic Actuators." 6715.1 (2007): 67150C-7150C-10. Web.
- [3] Del Vecchio, Ciro, Runa Briguglio, Armando Riccardi, and Marco Xompero. "Analysis of the Static Deformation Matching between Numerical and Experimental Data on the Voice-coil Actuated Deformable Mirrors." 9148 (2014): 914840-14840-7. Web.